ResearchGate

See discussions, stats, and author profiles for this publication at: https://www.researchgate.net/publication/224322940

Optimal control allocation in vehicle dynamics control for rollover mitigation

Conference Paper *in* Proceedings of the American Control Conference · July 2008

DOI: 10.1109/ACC.2008.4586990 · Source: IEEE Xplore

CITATIONS
52

READS
553

2 authors, including:

Tore Hägglund
Lund University
155 PUBLICATIONS **11,628** CITATIONS

SEE PROFILE

Some of the authors of this publication are also working on these related projects:

PID control View project

Closed-loop controlled anesthesia View project

All content following this page was uploaded by Tore Hägglund on 21 August 2014.

The user has requested enhancement of the downloaded file.

2008 American Control Conference
Westin Seattle Hotel, Seattle, Washington, USA
June 11-13, 2008

Optimal Control Allocation in Vehicle Dynamics Control for Rollover Mitigation

Brad Schofield and Tore Hägglund

Abstract— **Vehicle dynamics control systems, previously only intended for yaw stabilization, are now being extended to incorporate rollover mitigation via braking. Current systems typically use a heuristic approach to control allocation, often utilizing only a subset of the available actuators. In this article a computationally–efficient, optimization–based control allocation strategy is used to map controller commands to braking forces on all four wheels, taking into account actuator constraints. Simulations show that the strategy is capable of preventing vehicle rollover for various standard test manoeuvres.**

I. INTRODUCTION

The use of active safety systems in road vehicles is widespread, and most modern passenger vehicles are equipped with Anti–lock Braking Systems (ABS) to improve braking performance. Electronic Stability Programs (ESP), found in many modern vehicles, use the ABS hardware to stabilize yaw motion. The prevention of driver–induced, or 'untripped' rollover accidents however, requires a new form of active safety system. Such systems have been the topic of research for some years, and have recently found their way into production, in the form of ESP systems augmented with some rollover mitigation functionality. These production systems, as well as a number of the algorithms proposed in the literature, use individual wheel braking as actuators [1], [2], [3], [4]. Other algorithms have been proposed which utilize active steering, often in coordination with braking [5], [6]. The majority of these algorithms use a subset of the available actuators for control. Typically, in standard ESP systems, the front wheel on the outside of the turn is used, as this wheel experiences the most normal force due to load transfer. While this strategy is simple and often effective, ignoring the possibility of using other available actuators (the other wheels) reduces the achievable performance. In this article, optimization–based control allocation is used as a means of systematically determining braking commands for all wheels in order to achieve desired generalized force and moment commands generated by a vehicle dynamics controller. The resulting algorithm involves the online solution of a quadratic programming problem, as is done in Model Predictive Control (MPC). As with MPC, the algorithm is capable of handling actuator constraints. This allows for a high degree of fault tolerance, as faulty actuators can simply be removed from the optimization problem.

Brad Schofield and Tore Hägglund are with the Department of Automatic Control, Faculty of Engineering, Lund University, Box 118, SE 221 00 Lund, Sweden. {brad.schofield, tore.hagglund}@control.lth.se

II. OUTLINE

The tire and chassis models used in this article are outlined in Section III. A brief overview of the rollover mitigation control laws is given in Section IV; further details can be found in [7]. The derivation of the control allocation algorithm is presented in Section V. Simulation results obtained using DaimlerChrysler's proprietary vehicle simulation software are presented in Section VI.

III. VEHICLE MODEL

Vehicle models typically consist of two components, a chassis model which describes the dynamics of the vehicle, and a tire model which describes the forces generated at the contact point between the tire and the road. In order for a tire to produce a force, slip must occur. Longitudinal force F_x is produced by the longitudinal slip λ, and the lateral force F_y is produced by the lateral slip α. For small slip values, the relationships are approximately linear. For larger values, the forces saturate. The maximum achievable longitudinal force is given by $F_{x,max} = \mu F_z$, where μ is the coefficient of friction between the tire and the road and F_z is the normal force on the tire. The maximum available lateral force for a given lateral slip can be described by the so–called *Magic Formula* [8], which is a function of α and F_z. In the case of combined slip, where lateral and longitudinal slip occur simultaneously, a simple model for the resulting force is the *friction ellipse*, illustrated in Figure 1. The ellipse is described by the equation $\left(\frac{F_y}{F_{y,max}}\right)^2 + \left(\frac{F_x}{F_{x,max}}\right)^2 = 1$.

In order to adequately describe the dynamics of the vehicle, a nonlinear two–track model with roll dynamics can be used, as shown in Figure 2. Figure 3 illustrates the model in the vertical plane. The suspension is modelled as a torsional

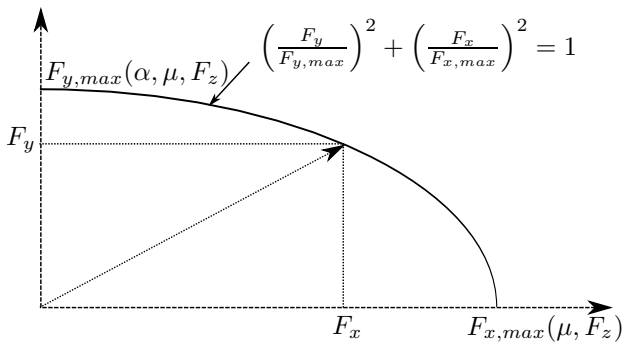

Fig. 1. The friction ellipse, showing maximum lateral and longitudinal forces, the resultant force and its components.

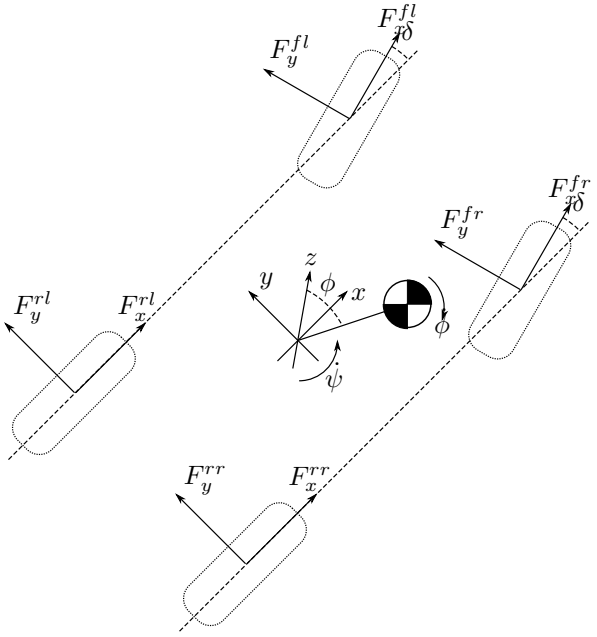

Fig. 2. Two-track model with roll dynamics.

spring–damper system, with roll stiffness C_ϕ and damping K_ϕ. The vehicle states are longitudinal velocity v_x, lateral velocity v_y, yaw rate $\dot{\psi}$, roll rate $\dot{\phi}$ and roll angle ϕ. The inputs to the system are the total longitudinal force F_{xT}, total lateral force F_{yT}, and total moment M_T. The relationships between these and the individual tire forces are derived in Section V. A full derivation of the model can be found in [7]. For the purpose of control, only the rotational dynamics are of interest. After some simplifications, the equations of rotational motion are found to be:

$$\ddot{\phi} = \frac{F_{yT}h + mgh\phi - C_\phi\phi - K_\phi\dot{\phi} + \dot{\psi}^2(I_{yy} - I_{zz})\phi}{I_{xx}} \quad (1)$$

$$\ddot{\psi} = \frac{M_T - F_{xT}h\phi - 2(I_{yy} - I_{zz})\phi\dot{\phi}\dot{\psi}}{I_{yy}\phi^2 + I_{zz}} \quad (2)$$

where m is the vehicle mass, h is the height of the centre of gravity above the roll axis, and I_{ii} is the moment of inertia abouth the ith axis.

IV. CONTROL DESIGN

A large number of different strategies for rollover mitigation have been proposed in the literature. One strategy, used by the authors [4], [7] as well as others [6], is to limit the roll angle while following a yaw rate reference trajectory. Restriction of the vehicle sideslip angle β (the angle between the vehicle-fixed x-axis and the velocity vector) is also important, but this can be accomplished through appropriate yaw rate control [9]. The control design is performed with respect to the generalized forces and moments, or *virtual controls* $v = \begin{pmatrix} F_{xT} & F_{yT} & M_T \end{pmatrix}^T$. These virtual controls are then mapped to actuator commands by the control allocator.

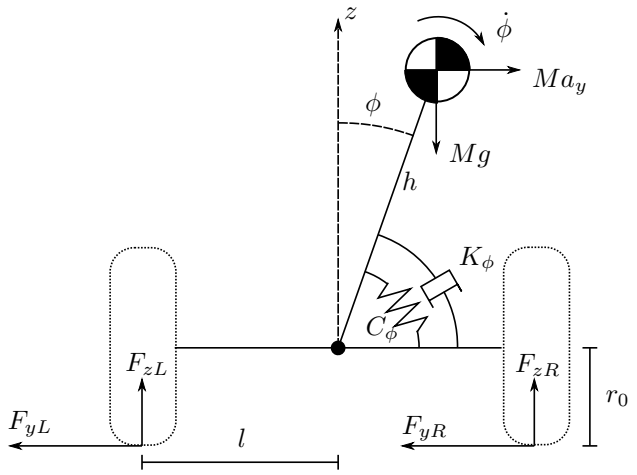

Fig. 3. The two-track model in the vertical plane, showing suspension modeled as a torsional spring and damper.

A. Roll Control

In [7] it was shown how a maximum allowable roll angle may be converted to a lateral acceleration limit. This allows the use of a control scheme based on the limitation of roll angle using lateral acceleration measurements only, at the cost of introducing a degree of parameter sensitivity, in particular to the centre of gravity height h. The lateral acceleration a_y is determined by the total lateral force F_{yT}. From the friction ellipse, it can be seen that F_{yT} can be influenced by varying the total longitudinal (braking) force F_{xT}. Therefore, F_{xT} will be used for roll control.

The strategy developed in [7] involves the use of a proportional–plus–derivative type filter for the lateral acceleration measurement used to trigger the controller, which is simply a predefined deceleration. Hysteresis is used to prevent chatterring. The use of a PD type filter is analogous to using both roll angle and rate information for switching, as is suggested in [5]. It can be interpreted as providing a prediction of the lateral acceleration over a certain horizon. This is important since it allows rapid activation of the controller. Let $\hat{a}_y(t)$ denote the filtered signal on which the switching is performed. Using the PD filter, $\hat{a}_y(t)$ may be obtained as:

$$\hat{A}_y(s) = K\left(A_y(s) + \frac{sT_d}{1 + sT_d/N}A_y(s)\right) \quad (3)$$

where $A_y(s)$ and $\hat{A}_y(s)$ are the Laplace transforms of $a_y(t)$ and $\hat{a}_y(t)$ respectively. T_d can be interpreted as the prediction horizon, and K is the static gain.

The resulting control law takes the form:

$$F_{xT} = \begin{cases} -m|a_x^d| & \text{if controller on} \\ 0 & \text{if controller off} \end{cases} \quad (4)$$

where a_x^d is the desired longitudinal acceleration. This may be obtained from the roll angle limit as in [7], or by empirical means. The controller is switched on when $|\hat{a}_y| \geq \hat{a}_y^{on}$ and off when $|\hat{a}_y| \leq \hat{a}_y^{off}$, where $\hat{a}_y^{on} > \hat{a}_y^{off}$ are predefined thresholds.

B. Yaw Control

Attention may now be directed at controlling the yaw rate $\dot{\psi}$. From (2), it can be seen that the yaw rate can be influenced by both M_T and F_{xT}. A simple Lyapunov function for the yaw dynamics is given by:

$$V_r(x,v) = \frac{1}{2}(\dot{\psi} - \dot{\psi}_{ref})^2 \tag{5}$$

By standard Lyapunov-based design, taking F_{xT} to be given by (4), M_T is found to be:

$$\begin{aligned} M_T =& (-K_r(\dot{\psi} - \dot{\psi}_{ref}) + \ddot{\psi}_{ref})(I_{yy}\phi^2 + I_{zz}) + F_{xT}h\phi \\ &+ 2\phi\dot{\phi}\dot{\psi}(I_{yy} - I_{zz}) \end{aligned} \tag{6}$$

For details see [7].

V. CONTROL ALLOCATION

The control laws derived in the previous section use the generalized forces F_{xT}, F_{yT} and M_T as virtual controls. The role of the control allocator is to obtain *actual controls* (in this case the individual braking forces) which will give rise to the desired virtual controls. Generally, the relationship is $v(t) = g(u(t))$ where $v(t) \in \mathbb{R}^k$ are the virtual controls, $u(t) \in \mathbb{R}^m$ are the actual controls and $g : \mathbb{R}^m \to \mathbb{R}^k$ is the mapping from actual to virtual controls, where $m > k$. The majority of the literature deals with the linear case [10], where the actual and virtual controls are related by a *control effectiveness matrix* B:

$$v(t) = Bu(t) \tag{7}$$

The control allocation problem is an under-determined, and often constrained problem. A common approach to solving these problems is to formulate an optimization problem in which the allocation error $||Bu(t) - v(t)||_2$ is minimized, subject to actuator constraints. The 2-norm of the allocation error is most commonly used.

A. Approximations

Since the controller will be operating exclusively in the limits of the vehicle's driving regime, it is reasonable to make approximations which are valid during these conditions. The first approximation is that the slip angles of all of the wheels are large enough such that the maximum lateral tire forces saturate, and are thus given by $F_{yi,max} = \mu F_{zi}$. This is attractive since the slip angles are not required in order to compute the maximum lateral forces. The resultant force on each wheel can now be seen as a function of the applied braking force and the normal force. However, the function is still nonlinear, so a further approximation is suggested to simplify the constraints. The friction ellipse can be approximated in each quadrant by a linear function, as in Figure 4. This approximation can be justified by considering that there will be a large amount of uncertainty in the radius of the friction circle. In particular, μ is highly uncertain. The linear approximation can be thought of as lying within circles defined by upper and lower bounds of the radius μF_z. The approximation may be refined by introducing tuning parameters to alter the gradient and position of the linear approximations, giving a relationship on the form:

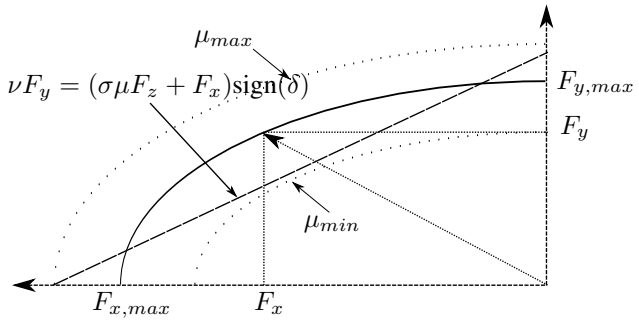

Fig. 4. The friction ellipse with linear approximation, showing the uncertainty regions arising from the uncertainty of μ. Note that the linear approximation is only valid for $-\sigma\mu F_z \leq F_x \leq 0$. The approximation must therefore be used with constraints to obtain reasonable results.

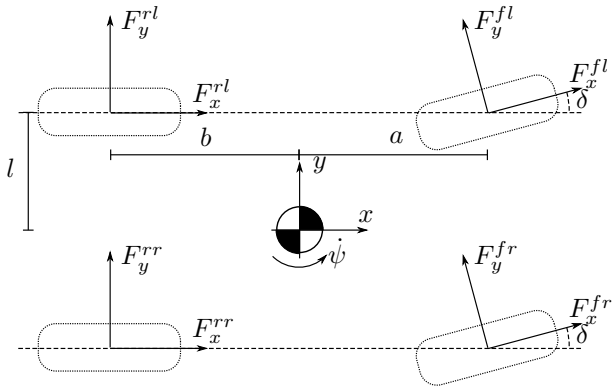

Fig. 5. Planar chassis model, showing the horizontal components of the tire forces.

$$\nu F_y = (\sigma\mu F_z + F_x)\text{sign}(\delta) \tag{8}$$

where ν and σ are tuning factors. The sign(δ) factor is required to ensure that the resultant force acts in the correct direction. This approximation has the attractive property that the constraints are convex. Using these simplifications, a control allocation problem can now be formulated.

B. Control Effectiveness Matrix Derivation

By considering Figure 5, the following expressions relating the individual tire forces to the generalized forces are obtained:

$$F_{xT} = F_x^{rl} + F_x^{rr} + (F_x^{fl} + F_x^{fr})\cos\delta - (F_y^{fl} + F_y^{fr})\sin\delta \tag{9a}$$

$$F_{yT} = F_y^{rl} + F_y^{rr} + (F_y^{fl} + F_y^{fr})\cos\delta + (F_x^{fl} + F_x^{fr})\sin\delta \tag{9b}$$

$$\begin{aligned} M_T =& (F_y^{fl} + F_y^{fr})a\cos\delta + (F_x^{fl} + F_x^{fr})a\sin\delta \\ &- (F_y^{rl} + F_y^{rr})b + (F_x^{rr} + F_x^{fr}\cos\delta + F_y^{fl}\sin\delta \\ &- F_x^{rl} - F_x^{fl}\cos\delta - F_y^{fr}\sin\delta)l \end{aligned} \tag{9c}$$

where δ is the steering angle (measured at the wheels). Replacing F_y with the linear approximation (8), the virtual

controls v can now be expressed as:

$$v(t) = B(\delta)u(t) + d(\delta)$$

where:

$$B(\delta) = \begin{pmatrix} \cos\delta - \frac{\Delta}{\kappa}\sin\delta & \frac{\Delta}{\kappa}\cos\delta + \sin\delta & b_M^1 \\ \cos\delta - \frac{\Delta}{\nu}\sin\delta & \frac{\Delta}{\nu}\cos\delta + \sin\delta & b_M^2 \\ 1 & \frac{\Delta}{\kappa} & -l - b\frac{\Delta}{\nu} \\ 1 & \frac{\Delta}{\nu} & l - b\frac{\Delta}{\nu} \end{pmatrix}^T$$

$$d(\delta) = \begin{pmatrix} -\frac{\sigma\mu\Delta\sin\delta}{\nu}(F_z^{fl} + F_z^{fr}) \\ \frac{\sigma\mu\Delta\cos\delta}{\nu}(F_z^{fl} + F_z^{fr}) + \frac{\sigma\mu\Delta}{\nu}(F_z^{rl} + F_z^{rr}) \\ d_M \end{pmatrix}$$

$$b_M^1 = (\frac{\Delta}{\nu}(a\cos\delta + l\sin\delta) + a\sin\delta - l\cos\delta)$$

$$b_M^2 = (\frac{\Delta}{\nu}(a\cos\delta - l\sin\delta) + a\sin\delta + l\cos\delta)$$

$$d_M = \frac{\sigma\mu\Delta}{\nu}\big[(a\cos\delta(F_z^{fl} + F_z^{fr}) + l\sin\delta(F_z^{fl} - F_z^{fr}) - b(F_z^{rl} + F_z^{rr})\big]$$

$$\Delta = \text{sign}(\delta)$$

$$u = \begin{pmatrix} F_x^{fl} & F_x^{fr} & F_x^{rl} & F_x^{rr} \end{pmatrix}^T$$

This can be transformed into the required form in (7) by defining new virtual controls $v'(t) = v(t) - d$. The constraints are now given by:

$$-|\sigma\mu F_{zi}| \leq F_{xi} \leq 0 \tag{10}$$

These constraints have the form of 'box constraints':

$$\underline{u} \leq u \leq \overline{u} \tag{11}$$

Note that the control effectiveness matrix is now a function of the steering angle δ. In conventional linear control design this would cause problems, but the use of control allocation alleviates this because the mapping is perfomed online at each sample instant. In the following, the dependence on δ will be dropped, and B regarded as a constant matrix.

A linearly-constrained quadratic programming problem may now be formulated. Such problems can take the form:

$$\begin{aligned} u &= \arg\min_{u\in\Omega} ||W_u(u - u_d)||_2 \\ \Omega &= \arg\min_{\underline{u}\leq u\leq\overline{u}} ||W_v(Bu - v')||_2 \end{aligned} \tag{12}$$

where W_u and W_v are diagonal weighting matrices, u_d is a desired actual control value, and $\underline{u}$ and $\overline{u}$ are constraints on the actual controls. This type of problem is known as Sequential Least-Squares (SLS), since the solution is computed in two steps. First, the weighted allocation error $||W_v(Bu - v)||$ is minimized. If feasible solutions are found, then the 'best' solution is obtained by minimizing $||W_u(u - u_d)||$. The desired actual control value u_d is zero in the results presented here, but may be chosen in other ways [10]. A faster algorithm can be obtained by approximating the SLS formulation as a Weighted Least-Squares (WLS) problem:

$$u = \arg\min_{\underline{u}\leq u\leq\overline{u}} \left(||W_u(u - u_d)||_2^2 + \gamma||W_v(Bu - v')||_2^2\right) \tag{13}$$

The parameter γ is typically chosen to be very large in order to emphasize the importance of minimizing the allocation error. In the results presented here, the WLS algorithm (13) has been used. Since only F_{xT} and M_T are used as virtual controls, F_{yT} may effectively be removed from the allocation problem by making the corresponding weight in the matrix W_v very small.

Such optimization problems can be solved by active set methods [10], [11]. Consider the least squares problem:

$$\min_u ||Au - b|| \tag{14a}$$

$$\text{subject to} \quad Bu = v \tag{14b}$$

$$\underbrace{\begin{pmatrix} I \\ -I \end{pmatrix}}_{C} u \geq \underbrace{\begin{pmatrix} \underline{u} \\ -\overline{u} \end{pmatrix}}_{U} \tag{14c}$$

The principal idea of active set methods is that in each step, some of the inequality constraints are taken to be equality constraints, while the remainder are ignored. Denote with $\mathcal{W}$ the *working set*, which contains all of the active constraints. The details of the active set algorithm used to solve the problem are given in Algorithm 1. Algorithm 2 shows how the WLS problem is solved.

Algorithm 1: Active set algorithm

Let u^0 be a feasible starting point, satisfying (14c) ;
for $i = 0, 1, 2, \ldots$ **do**
  Given suboptimal iterate u^i, find the optimal perturbation p, considering the inequality constraints in $\mathcal{W}$ as equality constraints and ignoring the remainder. This is done by solving:

$$\begin{aligned} &\min_p ||A(u^i + p) - b|| \\ &Bp = 0 \\ &p_i = 0, \quad i \in \mathcal{W} \end{aligned}$$

  if $u^i + p$ *feasible* **then**
    Set $u^{i+1} = u^i + p$;
    Compute Lagrange multipliers as:

$$A^T(Au - b) = \begin{pmatrix} B^T & C_0^T \end{pmatrix} \begin{pmatrix} \mu \\ \lambda \end{pmatrix}$$

    where C_0 consists of the rows of C corresponding to the constraints in the active set ;
    if $\lambda \geq 0$ **then**
      u^{i+1} is optimal solution;
      Return $u = u^{i+1}$
    else
      Remove constraint corresponding to most negative λ from the working set $\mathcal{W}$;
  else
    Find $\alpha^i = \max\{\alpha \in [0, 1] : \underline{u} \leq u^i + \alpha p \leq \overline{u}\}$ and set $u^{i+1} = u^i + \alpha^i p$. Add bounding constraint to active set.
end

Algorithm 2: Solution of the WLS control allocation problem (13)

Let u^0 be the optimal point obtained at time $t-1$, and $\mathcal{W}^0$ be the corresponding active set ;

if $\underline{u}(t) < u^0 < \overline{u}(t)$ **then**

Remove any active constraints from $\mathcal{W}^0$;

else

Saturate the infeasible elements of u^0 and update the initial working set $\mathcal{W}^0$;

Rewrite the cost function as:

$$||W_u(u-u_d)||_2^2 + \gamma||W_v(Bu-v')||_2^2 = \left\| \underbrace{\begin{pmatrix} \gamma^{\frac{1}{2}} W_v B \\ W_u \end{pmatrix}}_{A} u - \underbrace{\begin{pmatrix} \gamma^{\frac{1}{2}} W_v v \\ W_u u_d \end{pmatrix}}_{b} \right\|^2$$

Use Algorithm 1 to solve:

$$u = \arg \min_{\underline{u} \le u \le \overline{u}} ||Au - b||$$

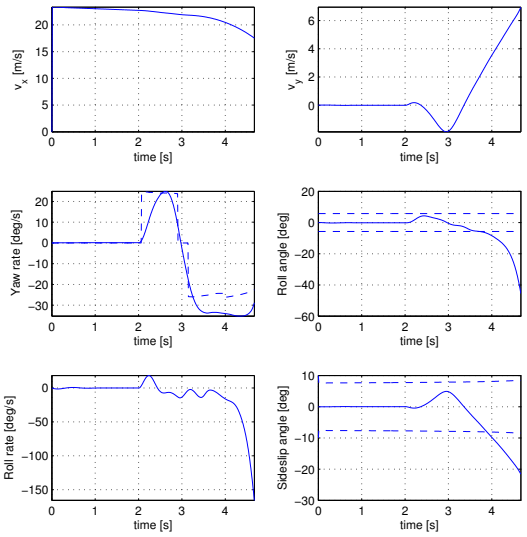

Fig. 6. Vehicle states with the controller inactive. The instability of the roll dynamics is evident. The simulation ceases to run after rollover occurs.

C. Rate Constraints

Rate constraints in the actuators (in this case the braking system) may be taken into account in the control allocation problem by modifying the constraints at each sample time. Let the rate constraints be given by $r_{min} \le \dot{u}(t) \le r_{max}$. After discretization, the maximum allowable deviations of the positions from one sample time to another are given by $\Delta_{min} = r_{min}T_s$ and $\Delta_{max} = r_{max}T_s$, where T_s is the sampling period. The position constraints may be rewritten as:

$$\underline{u}^*(t) = \max\{\underline{u}, u(t-Ts) + \Delta_{min}\} \quad (15)$$

$$\overline{u}^*(t) = \min\{\overline{u}, u(t-Ts) + \Delta_{max}\} \quad (16)$$

The rate constraints present in the control problem are the brake pressure rising and falling slew rates.

VI. SIMULATION RESULTS

The control strategy was simulated in Matlab/Simulink using DaimlerChrysler's proprietary CASCaDE (Computer Aided Simulation of Car, Driver and Environment). The vehicle used in the simulations was a light commercial van. A number of test maneuvers were simulated, including the J-turn, Fishhook and roll–rate feedback Fishhook. The results presented here correspond to the Fishhook manoeuvre.

A. Test Maneuver

The Fishhook manoeuvre is an important test manoeuvre in the context of rollover. It attempts to maximize the roll angle under transient conditions and is performed as follows, with a start speed of 80km/h[1]:

- The steering wheel angle is increased at a rate of 720deg/sec up to $6.5\delta_{stat}$, where δ_{stat} is the steering angle which is necessary to achieve 0.3g stationary lateral acceleration at 80km/h
- This value is held for 250ms
- The steering wheel is turned in the opposite direction at a rate of 720 deg/sec until it reaches -$6.5\delta_{stat}$

[1]The original specification from the NHTSA states a start speed of 50 mph.

B. Results

The controller was capable of preventing rollover in all of the test manoeuvres used. Figure 6 shows that rollover occurs when a Fishhook manoeuvre is performed with the controller inactive. Figure 7 shows the states of the vehicle when the controller is active. Rollover is prevented, with the roll angle and sideslip remaining within defined limits [7], and with reasonable yaw rate tracking.

Figures 8, 9 and 10 show the desired and achieved virtual control signals F_{xT}, M_T and F_{yT}. The 'predicted' virtual controls, corresponding to the virtual control values obtained using the allocator's model, are also displayed, and closely match the desired values. Although F_{yT} is not used by the controller, it is interesting to note that the actual value obtained closely corresponds to the value obtained from the allocator's model. This indicates that the approximations made in the tire model were reasonable.

VII. DISCUSSION AND CONCLUSIONS

A rollover prevention strategy based on limiting the roll angle has been presented. A key element of the strategy is the control allocator, which is capable of taking into account important actuator constraints while remaining sufficiently fast to be easily implemented in real–time.

Online optimization is used in a similar manner as in Model Predictive Control (MPC), which raises the question as to whether MPC based on linearized models could or should be used instead. There are however a number of

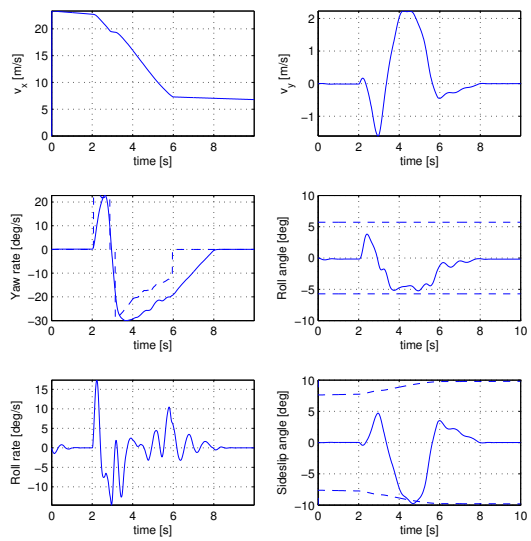

Fig. 7. Vehicle states with the controller active. The dashed lines are the yaw rate reference, maximum allowed roll angle and maximum sideslip angle respectively.

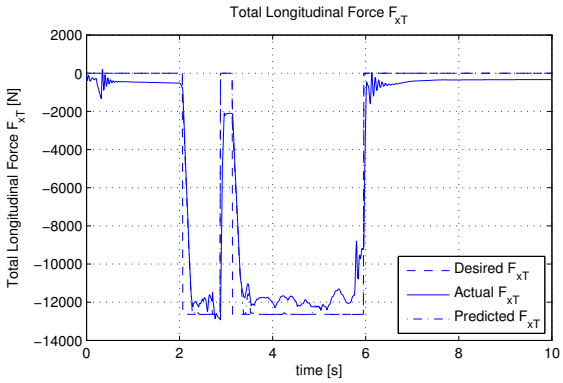

Fig. 8. Total longitudinal force F_{xT}.

obstacles to the use of MPC. Primarily, the relation between individual wheel forces and resultant forces and moments depends on the time-varying parameter δ. In order to use MPC, a multiparametric programming approach would be required. Additionally, the optimization problem obtained in the proposed method is tailored to the structure of the problem. Finally, the proposed method is arguably more intuitive, since the control design can be performed with the original physical models rather than linearized versions.

Additionally, the systematic approach gives a high degree of fault tolerance. Should an actuator fail, it is trivial to remove that actuator from the optimization problem.

VIII. ACKNOWLEDGMENTS

The authors would like to acknowledge the help of Dr. Jens Kalkkuhl, DaimlerChrysler AG. The work was carried out in the context of the Complex Embedded Automotive Control Systems (CEmACS) project, FP6-IST-004175.

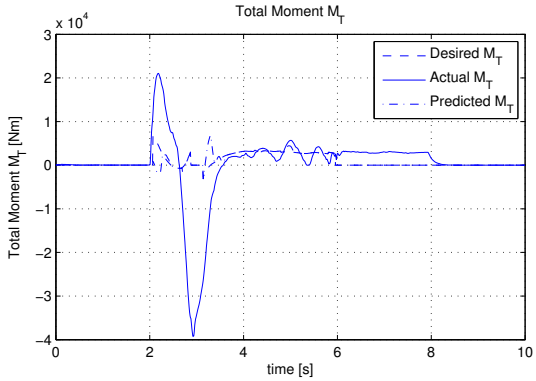

Fig. 9. Total moment M_T.

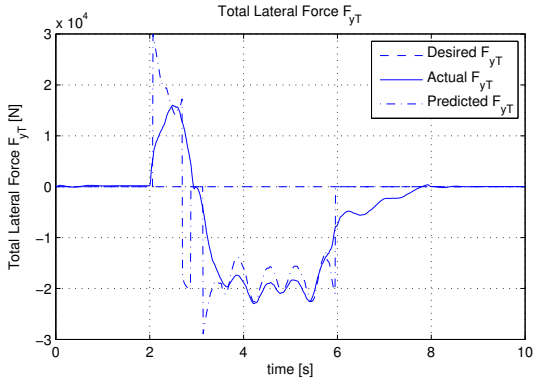

Fig. 10. Total lateral force F_{yT} .

REFERENCES

[1] B. Johansson and M. Gäfvert, "Untripped suv rollover detection and prevention," in *43rd IEEE Conference on Decision and Control*, 2004.

[2] B. C. Chen and H. Peng, "Rollover prevention for sports utility vehicles with human-in-the-loop evaluations," in *5th Int'l Symposium on Advanced Vehicle Control*, 2000.

[3] B. Chen and H. Peng, "Differential-braking-based rollover prevention for sport utility vehicles with human-in-the-loop evaluations," *Vehicle System Dynamics*, vol. 36, no. 4–5, pp. 359–389, 2001.

[4] B. Schofield, T. Hägglund, and A. Rantzer, "Vehicle dynamics control and controller allocation for rollover prevention," in *Proceedings of the IEEE International Conference on Control Applications*, Munich, Germany, Oct. 2006.

[5] D. Odenthal, T. Bunte, and J. Ackermann, "Nonlinear steering and braking control for vehicle rollover avoidance," 1999.

[6] C. R. Carlson and J. C. Gerdes, "Optimal rollover prevention with steer by wire and differential braking," in *Proceedings of the ASME International Mechanical Engineering Congress and Exposition*, Washington, D.C. USA, 2003.

[7] B. Schofield, "Vehicle dynamics control for rollover prevention," Department of Automatic Control, Lund University, Sweden, Licentiate Thesis ISRN LUTFD2/TFRT--3241--SE, Dec. 2006.

[8] H. B. Pacejka, *Tyre and Vehice Dynamics*. Butterworth Heinemann, 2002.

[9] P. Tøndel and T. A. Johansen, "Control allocation for yaw stabilization in automotive vehicles using multiparametric nonlinear programming," in *American Control Conference*, 2005.

[10] O. Härkegård, "Backstepping and control allocation with applications to flight control," Ph.D. dissertation, Department of Electrical Engineering, Linkping University, SE–581 83 Linkping, Sweden, May 2003.

[11] Å. Björck, *Numerical Methods for Least Squares Problems*. SIAM, 1996.

View publication stats